Structural and Functional Characterization of a Thioredoxin-Like Protein (Mt0807) from *Methanobacterium thermoautotrophicum*†

Godwin Y. Amegbey, Hassan Monzavi, Bahram Habibi-Nazhad, Sudeepa Bhattacharyya, and David S. Wishart*

Faculty of Pharmacy and Pharmaceutical Sciences, University of Alberta, Edmonton, Canada T6G 2N8

Received January 21, 2003; Revised Manuscript Received April 8, 2003

ABSTRACT: Mt0807 is an 85-residue thiol-redox protein from the anaerobic archaebacterium *Methanobacterium thermoautotrophicum*. Its small size, its participation in certain redox reactions, and the presence of a "classic" glutareodoxin active-site sequence have led to the suggestion that it might be a glutaredoxin. However, studies by previous workers indicated that it exhibited neither glutaredoxin-like nor thioredoxin-like properties. To clarify the true role of this protein and its structure/functional relationship with a paralogous thioredoxin (Mt0895, 28% sequence identity) and a recently characterized orthologous protein (Mj0307, 51% sequence identity), we undertook a series of biochemical and biophysical studies. Comparative enzymatic assays and thiol titration experiments were combined with NMR structural studies and detailed 3D structure comparisons. Structurally, our results show that Mt0807 has a glutaredoxin-like fold (central four-stranded β-sheet core surrounded by two helices on one side and a third on the other). However, more detailed comparisons with other members of the thioredoxin superfamily indicate that Mt0807 actually has several key structural and active-site characteristics more common to a thioredoxin. Furthermore, biochemical tests show that Mt0807 actually behaves as true thioredoxin. Comparisons between Mt0807 and its paralogue, Mt0895, indicate these two archaebacterial thioredoxins share very similar folds, but exhibit very different activities and likely serve somewhat different roles. On the basis of its greater relative abundance and significantly stronger redox activity, we believe that Mt0807 is the primary thioredoxin for *M. thermoautotrophicum*, while Mt0895 plays a minor or supportive role. We also suggest that these two molecules (Mt0807 and Mt0895) may represent a group of ancient proteins that were ancestral to both thioredoxins and glutaredoxins.

Thioredoxins and glutaredoxins are two classes of redox active proteins which are members of the thioredoxin superfamily. They take part in reactions such as redox control of transcription factors, electron transport to ribonucleotide reductase for the reduction of ribonucleosides, formation of disulfides in protein folding, or defense against oxidative stress and apoptosis (*1*−*5*).

Thioredoxins and glutaredoxins are characterized by having a common fold (the thioredoxin fold, a central four-stranded beta sheet flanked by three or four alpha helices) and an active site motif consisting of Cys−Xaa−Xaa−Cys, where Xaa corresponds to any naturally occurring amino acid (*6*, *7*). The cysteines in the active site, which undergo reversible disulfide exchange reactions with their respective substrates, are located at the N-terminus of a conserved alpha helix (*8*). In the reduced form, the N-terminal cysteine is generally solvent exposed and acts as a nucleophile, whereas the more C-terminal cysteine is buried (*9*). The difference between thioredoxin and glutaredoxin is that thioredoxin is reduced to the dithiol form by NADPH and thioredoxin reductase (the thioredoxin system), while glutaredoxin (*2*) is reduced by the tripeptide glutathione (GSH),[1] which in turn is reduced by NADPH and glutathione reductase (the glutaredoxin system). Thioredoxins and glutaredoxins can also be distinguished by their lack of cross reactivity with antibodies raised specifically against each protein (*10*). The protein coded by gene 0807 of *Methanobacterium thermoautotrophicum* (strain Marburg), a hyperthermophilic archaeon, has been shown by McFarlan and co-workers (*10*) to be a redox protein with an active site sequence similar to known glutaredoxins (-Cys−Pro−Tyr−Cys-) but with some properties inconsistent with either a glutaredoxin or a thioredoxin. Specifically, they reported that the protein does not function as a glutathione-disulfide oxidoreductase in the presence of glutathione/glutathione reductase, thereby suggesting it was not a glutaredoxin. However, they also found that even though it exhibited some thioredoxin-like properties, it was not a substrate for the thioredoxin reductase, thereby suggesting that it was not a true thioredoxin either.

† Financial Support: Protein Engineering Network of Centers of Excellence (PENCE) and the International Council for Canadian Studies (ICCS).

* To whom correspondence should be addressed. Tel: 780-492-0383. Fax: 780-492-5305. E-mail: david.wishart@ualberta.ca.

[1] Abbreviations: CE, combinatorial extension; DSS, 2,2-dimethyl-2-silapentane-5-sulfonic acid; DTNB, 5,5′-dithiobis (2-nitrobenzoic acid); DTT, dithiothreitol; EDTA, ethylenediamine tetraacetic acid; FAD, flavin adenine dinucleotide; GSH, glutathione; HSQC, heteronuclear single quantum coherence spectroscopy; $NADP^+$, nicotinamide adenine dinucleotide phosphate (oxidized); NADPH, nicotinamide adenine dinucleotide phosphate (reduced); NMR, nuclear magnetic resonance; NOE, nuclear Overhauser effect; NOESY, nuclear Overhauser effect spectroscopy; PDI, protein disulfide isomerase; RMSD, root mean square deviation; SCOP, structural classification of proteins; TOCSY, total correlation spectroscopy.

10.1021/bi030021g CCC: $25.00
Published on Web 06/11/2003

Recent whole genome analyses of various hyperthermophilic organisms (*11*−*17*) as well as NrdH proteins isolated from mesophilic organisms (*5*, *18*) have revealed that there are classes of small redox proteins that have sequences and folds similar to glutaredoxins but which have true thioredoxin-like activities (*19*−*21*). Most interestingly, studies by Bhattacharyya et al. (*20*) have revealed the presence of another paralogous thioredoxin (Mt0895) in *M. thermoautotrophicum* that shares 28% sequence identity to Mt0807. Additionally, work by Lee et al. (*19*) has demonstrated true thioredoxin activity for a small redox protein from *Methanococcus jannaschii* (Mj0307) which has 51% sequence identity to Mt0807.

To clarify the role of Mt0807 and its relationship (both structural and functional) to its paralogue Mt0895, we undertook additional biochemical/biophysical tests on Mt0807. We have also determined its solution structure via NMR to explore the structure−function relationship between Mt0807 and Mt0895. Our findings show that Mt0807, despite having a classic glutaredoxin active site sequence (-Cys−Pro−Tyr−Cys-) and a classic glutaredoxin fold, is actually a true thioredoxin. Sequence comparisons, detailed structural analyses of the charge distribution around the active site, as well as enzymatic assays (which employed a more sensitive two-step redox activity assay than used by previous workers (*10*)) clearly indicate that Mt0807 is similar to other known thioredoxins from Archaea. Our data also show that Mt0807 is more oxidizing than its paralogue Mt0895, even though the two proteins have very similar structures and appear to use the same reducing system.

MATERIALS AND METHODS

Protein Expression, Purification, and Sample Preparation. The Mt0807 gene was provided by professor Cheryl Arrowsmith of the division of Molecular and Structural Biology, Ontario Cancer Institute (Toronto, Canada). The gene was subcloned into a pET15b vector (Novagen) and transformed into a BL21 (DE3) strain of *Escherichia coli* for expression. The vector expresses the protein with an N-terminal hexahistidine tag followed by a thrombin cleavage site. Protein expression was accomplished by growing the transformed *E. coli* cells in a minimal (M9) growth medium. Uniform isotopic enrichment with ^{15}N or $^{15}N/^{13}C$ was accomplished by substituting the NH_4Cl and/or glucose in the M9 medium with $^{15}NH_4Cl$ and [U-^{13}C]-glucose (Martek Labs, Richmond, VA), respectively. Cells were grown at 37 °C in shaker flasks to an optical density of 0.6 and then induced with isopropyl-β-D-thiogalactopyranoside (IPTG) to a final concentration of 1 mM. The cells were allowed to grow for an additional 8 h before harvesting and centrifugation. Cell pellets were resuspended in a lysis buffer (50 mM $NaHPO_4$, 300 mM NaCl, 10 mM imidazole, pH 8.0) using 5 mL of the buffer per gram (wet weight) of cell pellet. Lysozyme was added to a concentration of 10 μg/mL. The mixture was then incubated in dry ice for 30 min and thawed in a water bath at 37 °C for 30 min. This freeze−thaw process was repeated three times. The lysed cells were then centrifuged at 15 000 rpm for 90 min at 4 °C. The supernatant was isolated, and RNase and Dnase 1 were added to a concentration of 10 μg/mL. The mixture was incubated at room temperature for 10 min and centrifuged at 15 000 rpm for 45 min. The protein was then purified in the native condition using the nickel nitrilotriacetic acid-agarose resin (Ni−NTA) column (Qiagen) as described elsewhere (*22*). The histidine tag was not cleaved from the protein as this type of tag does not interfere with the spectral properties or functional activities of the protein (*77*, *78*).

NMR Spectroscopy. NMR samples were prepared by dissolving about 6 mg of protein in 500 μL of a buffer solution (pH 6.0) made up of 50 mM NaH_2PO_4, 100 mM NaCl, 50 μL of D_2O, 1 mM DSS, and 10 μL of a 3% solution of sodium azide. NMR experiments were recorded at 25 °C on a Varian Inova 500 MHz spectrometer equipped with a 5-mm triple resonance and pulse gradient accessories. Two-dimensional ^{1}H-NOESY (mixing times of 80 ms and 150 ms), 2-D ^{1}H-TOCSY (mixing time of 60 ms) experiments were acquired on the unlabeled sample (*23*, *24*). Additionally, ^{1}H-^{15}N HSQC, ^{1}H-^{15}N NOESY−HSQC (mixing time 80 and 150 ms), and ^{1}H-^{15}N TOCSY−HSQC (mixing times of 50 and 100 ms) experiments were collected on the ^{15}N-labeled sample (*24*, *25*). In addition, HNCO (*26*) and HNCACB (*27*) data were collected on the $^{15}N/^{13}C$ labeled sample. All spectra were processed with an in-house spectral processing program (PROSIGN), which is a menu driven package written specifically for the Varian VNMR environment.

Assignments and Experimental Restraints. Sequential chemical shift assignments for Mt0807 were obtained by identifying $^{13}C\alpha$(i) to $^{13}C\alpha$ (i-1) and $^{13}C\beta$(i) to $^{13}C\beta$(i-1) connectivities from the HNCACB spectrum. The backbone chemical shift assignment was then completed using data from HNCO and ^{1}H-^{15}N TOCSY−HSQC spectra. Side chain ^{1}H assignments of each amino acid was then added using the ^{1}H-^{15}N HSQC (Figure 1) and spin systems obtained from the ^{1}H-^{15}N TOCSY−HSQC spectra. Stereospecific assignments of $^1H\beta$ protons were based on the intensities of ^{1}HN-$^1H\beta$ and $^1H\alpha$-$^1H\beta$ cross-peaks in the ^{1}H-^{15}N NOESY−HSQC and 2-D ^{1}H−NOESY spectra. The methyl groups of Val and Leu were assigned stereospecifically based on the intensity of ^{1}HN-$^1H\gamma$, $^1H\alpha$−$^1H\gamma$ cross-peaks. NOE distance restraints were obtained from the ^{1}H-^{15}N NOESY−HSQC and 2-D ^{1}H−NOESY spectra. NOE peak intensities were obtained from the volume integration of well resolved cross-peaks. Assigned NOE restraints were classified into three distance ranges: 1.8−2.7 Å, 1.8−3.5 Å, and 1.8−5.0 Å corresponding to strong, medium, and weak NOE intensities, respectively. Torsion angle constraints were predicted using an in-house program called SHIFTOR (*28*), which calculates both the phi and psi torsion angles from observed ^{1}HN, $^1H\alpha$, $^{13}C\alpha$, $^{13}C\beta$, and ^{13}CO chemical shifts. Hydrogen bond restraints (d_{O-HN} = 1.6−2.4 Å and d_{O-N} = 2.6−3.4 Å) were identified from the pattern of sequential and inter-strand NOEs involving amide and alpha protons and from the chemical shift index (*29*).

Structure Calculations. Structures for Mt0807 were calculated using X-PLOR version 3.851 (*30*). Sixty random structures were generated using X-PLOR's standard simulated annealing protocol for NMR structure determination (*31*, *32*). Only NOE-derived internuclear distance constraints representing the secondary structure elements were used (*33*). These random structures were then regularized using the distance geometry/simulated annealing protocol (dgsa.inp) (*32*, *34*, *35*) of X-PLOR with additional sets of NOE constraints. The regularization stage was repeated after correcting NOE distance violations (usually by extending

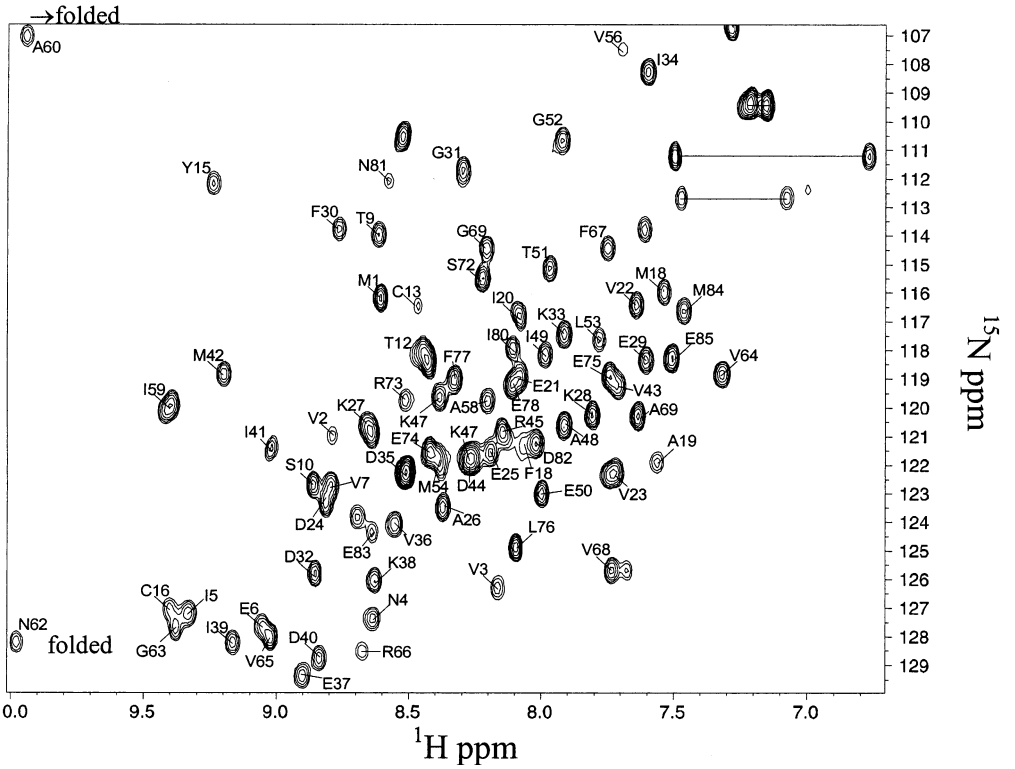

FIGURE 1: ^{1}H-^{15}N HSQC spectrum from 1 mM Mt0807 in 500 μL of a buffer solution made of 50 mM NaH_2PO_4, 100 mM NaCl, 50 μL of D_2O, 1 mM DSS pH 6.0 and 10 μL of a 3% solution of sodium azide, collected on Varian Inova 500 MHz spectrometer.

their upper distance limits) after visually reassessing the corresponding NOE spectral intensities. Typically these problem NOEs were borderline cases falling between the strong/medium or medium/weak NOE intensity categories. Dihedral angle and hydrogen bond restraints were then introduced and the structures were further refined using X-PLOR's simulated annealing refinement (refine.inp) protocol for NMR structure determination (*34*). A total of 997 restraints (comprising of 214 intraresidue NOEs, 659 interresidue NOEs (345 sequential, 187 medium range and 127 long range), 82 dihedral angle restraints and 42 hydrogen bonds) were used for the structure calculations. The final set of 20 structures was selected based on the acceptance criteria that no interproton distance violation could be more than 0.5 Å, no torsion angle, bond angle, or improper dihedral angle restraint violation could be greater than 5.0° and no bond violation could be greater than 0.05 Å. The dihedral angle and NOE-(distance)-refined structures were further refined using the mini_shift_coup.inp protocol of X-PLOR (*36*−*38*). This protocol refines the structures based on NOE distance, dihedral angle, and chemical shift restraints. The refined structures were analyzed with PROCHECK−NMR (*39*) and VADAR (*40*). MOLMOL (*41*) was used to visualize all the structures (Figure 2a,b) and to calculate the RMSD values.

Measurement of Thiol Ionization in Mt0807 by Ultraviolet Absorbance. Thiol Ionization constants for Mt0807 were measured using the protocol of Dyson et al. (*42*). Fresh samples of Mt0807 (1.0 mL of a 1 mM sample in 0.1 M potassium phosphate, 0.1 mM EDTA, pH 7.0 under argon) was reduced using 1.0 mL of a 10 mM DTT. Excess DTT was removed by dialysis against the same buffer under an argon atmosphere. After dialysis, the protein sample was diluted to a concentration of about 30 μM in a 0.1 mM

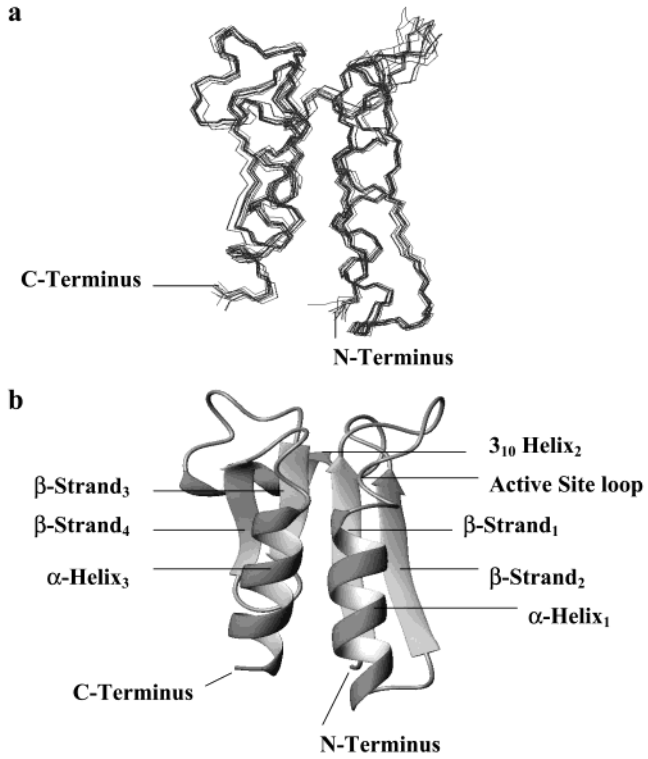

FIGURE 2: (a) A stereoview of the MOLMOL superposition of backbone atoms from the 20 best calculated structures. (b) Ribbon diagram of a representative structure of Mt0807.

EDTA, and 100 mM potassium phosphate buffer (pH 6.0). Thiol ionization was monitored by measuring the protein absorbance at 240 nm on a Pharmacia Biotech Ultraspec 3000 UV/Vis spectrophotometer. Small aliquots of 1.0 M NaOH or 2.0 M HCl were added to adjust the pH up or down. After each addition, the change in protein concentra-

Table 1: Structural Statistics for Mt0807: (Final 20 Models)

total restraints used	997
total noe restraints	863
intraresidue	214
sequential ($\|i-j\| = 1$)	345
medium range ($1 < \|i-j\| < 5$)	187
long range ($\|i-j\| > 4$)	127
no. hydrogen bonds	42
no. dihedral restraints	82
coordinate precision (angstroms)	
RMSD of all backbone atoms	0.55 ± 0.21 Å
RMSD of all heavy atoms	1.09 ± 0.33 Å
procheck nmr statistics	
residues in most favored region	67.0%
residues in additional allowed region	30.6%
residues in generously allowed region	1.3%
residues in disallowed region	1.1%

tion was noted at 280 nm. The concentration of Mt0807 was calculated at 280 nm using an extinction coefficient of 3230 M^{-1} cm^{-1}.

Measurement of Thioredoxin/Glutaredoxin activity. Thioredoxin/Glutaredoxin activity measurements were performed using the method described by Holmgren (*43*). To assay for glutaredoxin activity, a solution containing 750 μL of 100 mM Tris HCl (pH 8.0) with 1 mM EDTA, 0.35 mM NADPH, 1 mM glutathione, and 0.75 nM yeast glutathione reductase (Sigma, St. Louis, MO) was prepared. After 5 min of equilibration, a quantity (20 μL of 0.2 mM) of either Mt0807, Mt0895, *E. coli* thioredoxin (Sigma), *E. coli* glutaredoxin (Sigma), or T4 glutaredoxin (*44*) was added to the reaction mixture and the change in absorbance was monitored at 340 nm. To assay for thioredoxin activity, a solution containing 750 μL of 100 mM Tris HCl (pH 8.0) with 1 mM EDTA, 0.35 mM NADPH, and 0.02 mM of either Mt0807, Mt895, T4 glutaredoxin, or *E. coli* thioredoxin was prepared. After allowing the solution to equilibrate for 3 min, 20 μL of a 0.01 mM solution of *E. coli* thioredoxin reductase (Sigma) was added and the oxidation of NADPH was monitored at 340 nm using a Pharmacia Biotech Ultraspec 3000 UV/Vis spectrophotometer. After 25 min, 40 μL of a 10 mM solution of DTNB (5,5′-dithiobis (2-nitrobenzoic acid)) was added and the change in absorbance at 412 nm was further monitored.

RESULTS

Solution Structure. Statistical parameters for the ensemble of 20 calculated structures are presented in Table 1. All the structures (Figure 2a) show good covalent geometry as indicated by a low RMSD from idealized values and by low NOE, dihedral angle, and van der Waals energies. The refined structures were analyzed with PROCHECK−NMR (*39*), which indicated that for all 20 structures, 99.0% of the main chain (ϕ,ψ) angles fall into the allowed regions of the Ramachandran map. With the exception of the active site loop, (residues 12−16) and the C-terminus (residues 84−85), all portions of the Mt0807 structure are well-defined by NMR standards. The complete set of 20 Mt0807 structures has been deposited with the Protein Data Bank (PDB accession: 1NHO). The complete set of ^{1}H, ^{13}C, and ^{15}N chemical shifts has been deposited with the BioMagResBank (BMRB accession number: 5622). Visual inspection of the structure shows that Mt0807 is made up of a four-stranded β-sheet sandwiched between two helices on one side and a third on the other (Figure 2b). The β-sheets have a $\uparrow\beta_4\downarrow\beta_3\uparrow\beta_1\uparrow\beta_2$ orientation with helices 1 and 3 packing against each other on one side of the β-sheet and helix 2 on the other. The four β-strands in Mt0807 include residues 3−8 (strand β_1), 34−39 (strand β_2), 58−61 (strand β_3), and 65−68 (strand β_4). The first helix (α-helix$_1$) is the longest and runs from residue 19−30. The third helix (α-helix$_3$) is on the same side of the sheets as α-helix$_1$ and is composed of residues 74−84. The second helix (residues 45−50) exhibits properties of a 3_{10} helix and connects strand β_2 to β_3. Despite having "helical" chemical shifts, this 3_{10} helix was found to have the characteristic Hα(i)−HN(i + 2) NOE connectivities along its length and was marked by an absence of Hα(i)−HN(i + 4) NOE interactions (*33*). The presence of a 3_{10} helix was also confirmed by the secondary structure analysis of the final protein structures with MOLMOL (*41*) and VADAR (*40*). Another structural feature characteristic of the thioredoxin/glutaredoxin fold includes a cis-peptide bond (preceding strand β_3) at Pro 57 (*6*). The presence of this cis-peptide bond was confirmed by the characteristic Hα(i)−Hα(i + 1) and HN(i)−Hα(i + 1) NOE connectivities (*33*). Additionally, the side chain of Phe 8 is found to pack into a hydrophobic pocket formed by the N-terminus of α-helix$_2$ and it is highly conserved in all disulfide oxido-reductases as either a tyrosine or a phenylalanine residue (*45*). The topological arrangement of the secondary structural elements ($\beta-\alpha-\beta-\alpha-\beta-\beta-\alpha$) and the overall 3D structure clearly indicates that Mt0807 has a glutaredoxin-like fold (*2*) as has been found for other members of the archaeabacterial redox protein family (*19*, *20*).

Sequence and Structural Comparison with Other Thioredoxins and Glutaredoxins. Primary sequence analysis was conducted on Mt0807 using PSI−BLAST (*72*). Results obtained from the database search clearly show that Mt0807 belongs to the thioredoxin/glutaredoxin superfamily. It shows relatively high sequence identity with orthologous members in the Archaea family (ranging from between 51−28%) and also with the bacterial thioredoxins/glutaredoxins. However, the level of sequence identity of Mt0807 to the well-characerized members of the thioredoxin superfamily rarely exceeded 20%. Primary sequence alignment based on structural alignments obtained from the Combinatorial Extension (*71*) database was done on Mt0807 using representative structures from the thioredoxin/glutaredoxin superfamily. The structures included: thioredoxin H from *Chlamydomonas reinhardtii* (1TOF), thioredoxin from *E. coli* (1XOB), Human thioredoxin (4TRX), thioredoxin from *M. jannaschii* (1FO5), thioredoxin from *M. thermoautotrophicum* (1ILO), glutaredoxin from *E. coli* (1EGR), and human glutaredoxin (1JHB). The result is shown in Figure 3 and it indicates that even though the sequence identities might be low, the secondary structure however is very much conserved. These results also show that the active site sequence in Mt0807 is a classic (−Cys−Pro−Tyr−Cys-) glutaredoxin active-site sequence.

A qualitative structural comparison was carried out between Mt0807 and other representative members of the thioredoxin/glutaredoxin superfamily including: (i) T4 glutaredoxin (1DE1); (ii) thioredoxin (*E. coli*, 1XOB); (iii) glutaredoxin-1 (*E. coli*, 1EG0); (iv) human glutaredoxin (1JHB); (v) human thioredoxin-like (1GH2); (vi) thioredoxin Mt0895 (1ILO) and (vii) thioredoxin Mj0307 (1F05). This

FIGURE 3: Structure-based sequence alignment of Mt0807, thioredoxin H from *Chlamydomonas reinhardtii* (1TOF), thioredoxin from *E. coli* (1XOB), human thioredoxin (4TRX), thioredoxin from *M. thermoautotrophicum* (1ILO), thioredoxin from *M. jannaschii* (1FO5), glutaredoxin from *E. coli* (1EGR), and human glutaredoxin (1JHB). The β-strands and α-helices are marked gray. The 100% conserved residues are enclosed in a box.

Table 2: Protein Structures Similar to Mt0807 Derived from the SCOP Database

protein	Z score	RMSD	alignment length	sequence length	no of gaps	PDB code
thioredoxin Mt0895 (*Methanobacterium thermoautotrophicum*)	8.58	2.9	60	77	5	1ilo
thioredoxin Mj0307 (*Methanococcus jannaschii*)	8.47	3.2	69	85	6	1fo5
glutaredoxin (*Escherichia coli*)	8.40	3.3	64	85	6	1egr
glutaredoxin (Bacteriophage T4)	8.31	3.3	64	87	7	1de2
thioredoxin H (*Chlamydomonas reinhardtii*)	8.0	3.5	74	112	4	1tof
thioredoxin-like (2Fe-2S) ferredoxin (*Aquifex aeolicus*)	7.8	3.2	64	109	6	1f37
glutaredoxin (Bacteriophage T4)	7.6	3.4	65	87	6	1aaz
glutathione transferase P1−1 (*Homo sapiens*)	7.5	3.7	67	209	5	1eoh
glutathione transferase P1−1 complexed with cibacron blue (*Homo sapiens*)	7.4	3.7	66	208	6	20gs
thioredoxin (*Homo sapiens*)	7.4	3.3	71	105	5	3trx

detailed visual analysis revealed obvious similarities among all the structures as expected for the glutaredoxin/thioredoxin superfamily. One difference of note between the structure of Mt0807 and the standard glutaredoxin fold is the connection between β_4 and α_3. In the archaebacterial redox proteins, this connection is made up of between 4 and 6 residues, whereas this junction in *E. coli* glutaredoxin-1 (and all mesophilic prokaryotic or eukaryotic glutaredoxin structures) is rather short, typically consisting of a single glycine residue (*45*). Therefore, this loop is more similar to that of *E. coli* thioredoxin. Also helix$_2$ is considerably shorter in archaebacterial redox proteins than in glutaredoxins but comparable to that of thioredoxin from *E. coli*. It was also observed that the connection between β_2 and α_2 is much shorter than in *E. coli* glutaredoxin but comparable to that of *E. coli* thioredoxin. A hydrophobic pocket at the surface and the loop between α_2 and β_3 is a common determinant in all other thiol redoxins, for the recognition and binding of thioredoxin to thioredoxin reductase. This loop occupies a complementary groove on the surface of thioredoxin reductase upon binding (*46*). In Mt0807, this loop (residues 51−56) occupies a similar position and orientation when Mt0807 and the other thioredoxin-like proteins are superimposed—much more so than when it is superimposed with *E. coli* glutaredoxin. At the C-terminal end of β_4 is glycine residue (Gly69 in Mt0807), which is highly conserved in the thioredoxin superfamily (*47*). This residue has been shown to be important in binding of thioredoxin to other molecules such as T7 DNA polymerase, thioredoxin reductase (*48*), or in the assembly of filamentous phages (*49*). One unique difference between the structure of Mt0807 and that of the other known oxido-reductase proteins is that helix$_2$ is a 3_{10} helix in Mt0807, whereas it is an alpha helix in the others. More quantitative comparison of the structure of Mt0807 with other known thioredoxins/glutaredoxins was also achieved by submitting the representative structure of Mt0807 to be searched against the PDB, Dali (*68*, *69*), SCOP (*70*), and CE (*71*) databases. The results are listed in Table 2 and commented on in the discussion section.

Thiol Ionization by UV Spectroscopy. The thiol ionization measurement of the pK_a is based on the principle that the thiol (−SH) and the thiolate ion ($-S^-$) absorbs UV light to different extents at a wavelength of 240 nm with a difference in extinction coefficient of about 4000 M^{-1} cm^{-1} (*50*−*52*). This extinction coefficient difference is sufficiently high to permit facile monitoring of thiol ionization without interference from peptide absorption bands at 200−220 nm or aromatic absorption bands at 260 nm. Figure 4 shows the result of the thiol ionization test conducted on Mt0807. A titration is clearly visible with a midpoint at ~pH 6.2 and a

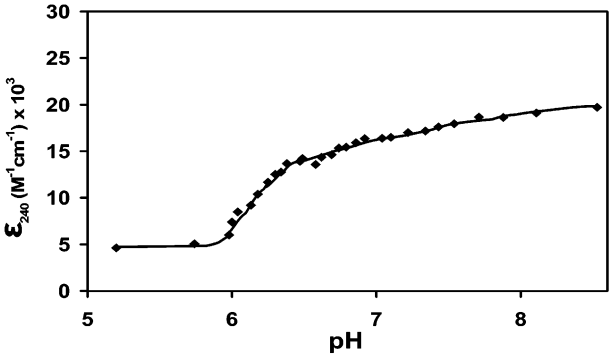

FIGURE 4: Measurement of thiol ionization in Mt0807 by ultraviolet absorbance at 240 nm. The ϵ_{240} (extinction coefficient at 240 nm) from pH 5.0 to 10.0 of a solution of Mt0807 containing 30 μM protein was recorded in 0.1 mM EDTA and 100 mM potassium phosphate buffer.

change in extinction coefficient of about 7900 M^{-1} cm^{-1} between pH 5.90 and 6.40, corresponding to two thiols titrating at the same pH. Fitting this value to the Henderson−Hasselbach equation gives an approximate pK_a of 6.23 for both Cys13 and Cys16 in the active site of the enzyme. The curve also shows other groups possibly titrating in the basic medium, although this may be due to the partial unfolding of the protein at high pH (*42*).

Thioredoxin Activity. Thioredoxin reductase specifically reduces oxidized thioredoxin to reduced thioredoxin using NADPH. The reduced thioredoxin forms a powerful protein disulfide reductase and spontaneously reduces other oxidized proteins. This is expressed in eqs 1 and 2 below and it describes the principle behind all thioredoxin/thioredoxin reductase assays (*53*).

$$\underset{\text{oxidized thioredoxin}}{\text{Trx}-S_2} + \underset{\text{reduced NADPH}}{\text{NADPH}} + H^+ \xrightleftharpoons{\text{thioredoxin reductase}} \underset{\text{reduced thioredoxin}}{\text{Trx}-(SH)_2} + \underset{\text{oxidized NADPH}}{NADP^+} \quad (1)$$

$$\underset{\text{reduced thioredoxin}}{\text{Trx}-(SH)_2} + \underset{\text{oxidized protein}}{\text{Protein}-S_2} \xrightarrow{\text{spontaneous}} \underset{\text{oxidized thioredoxin}}{\text{Trx-}S_2} + \underset{\text{reduced protein}}{\text{Protein}-(SH)_2} \quad (2)$$

Thioredoxin reductase is an FAD-containing enzyme and functions by transferring reducing equivalents to a disulfide bond in the active site of a redox protein via FAD. The thioredoxin reductase subunits contains FAD and NADPH binding domains and studies suggest that thioredoxin reductase must undergo a large conformational change during enzyme catalysis for oxidized thioredoxin to be reduced by the dithiol of the reduced enzyme (*54*). *E. coli* thioredoxin reductase is specific for its homologous oxidized thioredoxin molecule, but it also shows reactivity with other thioredoxin molecules from other organisms (*53*). The results of the thioredoxin activity assay for Mt0807 indicate that the first part (Figure 5b) of the two-step reaction is occurring in all the proteins used in the test. This indicates that thioredoxin reductase is reducing the proteins and Mt0807 is by far the most oxidizing protein of the protein molecules tested. The second step (Figure 5c) seems to be nonexistent for Mt0807, while T4 glutaredoxin and *E. coli* thioredoxin showed the highest activity and Mt895 shows only moderate activity. It is worth noting here that T4 glutaredoxin is the only redox protein reported to have both glutaredoxin and thioredoxin activity (*10*, *55*). Our results suggest that even though Mt0807 is showing a very strong interaction with *E. coli* thioredoxin reductase, it lacks the spontaneous reduction activity observed for many thioredoxin-like molecules in its class. Mt0807 is, therefore, more of an oxidizing protein than a reducing one. This is manifested by its low pK_a value and may also be related to the very reducing environmental niche that *M. thermoautotrophicum* occupies (*8*, *19*, *56*).

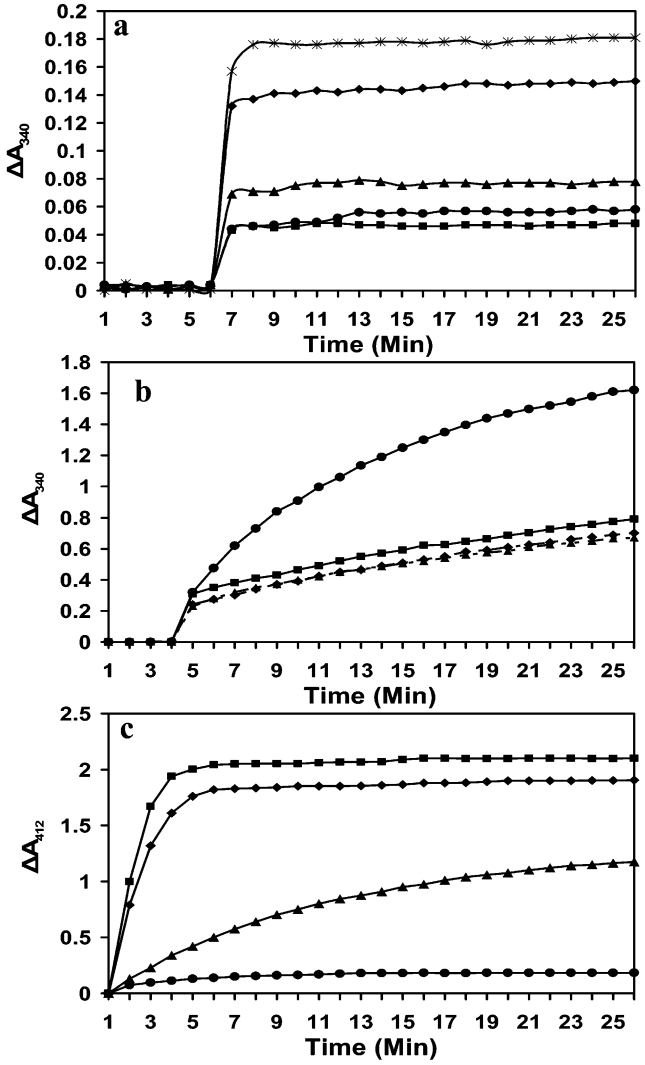

FIGURE 5: Measurement of thioredoxin and glutaredoxin activity via ultraviolet absorbance (a) Glutaredoxin activity kinetics. The ΔA_{340} (change in absorbance at 340 nm) for T4 glutaredoxin (*), *E. coli* glutaredoxin (◆), *E. coli* thioredoxin (■) Mt0895 (●) and Mt0807 (▲). (b) Thioredoxin activity kinetics (oxidation of NADPH). The ΔA_{340} (change in absorbance at 340 nm) for T4 glutaredoxin (■), *E. coli* thioredoxin (◆), Mt0895 (▲) and Mt0807 (●). (c) Thioredoxin activity kinetics (reduction of DTNB). The ΔA_{340} (change in absorbance at 340 nm) for T4 glutaredoxin (■) *E. coli* thioredoxin (◆), Mt0895 (▲), and Mt0807 (●).

Glutaredoxin Acivity. Glutaredoxin activity is shown by Holmgren (*57*) as a two-step reaction as indicated by eqs 3 and 4 below.

$$\underset{\text{oxidized glutaredoxin}}{\text{glutaredoxin-}S_2} + \underset{\text{reduced glutathione}}{2\text{GSH}} \rightarrow \underset{\text{reduced glutaredoxin}}{\text{glutaredoxin-}(SH)_2} + \underset{\text{oxidized glutathione}}{\text{GSSG}} \quad (3)$$

$$\underset{\text{oxidized glutathione}}{\text{GSSG}} + \underset{\text{reduced NADPH}}{\text{NADPH}} + H^+ \xrightarrow{\text{glutathione reductase}} \underset{\text{reduced glutathione}}{2\text{GSH}} + \underset{\text{oxidized NADPH}}{NADP^+} \quad (4)$$

The glutaredoxin activity test, therefore, should depend on the ability of the redox protein to bind and oxidize glutathione. Figure 5a shows the results of this test for T4 glutaredoxin, *E. coli* glutaredixin, *E. coli* thioredoxin, Mt0895, and Mt0807. The glutaredoxin activity observed for Mt0807 is more than that observed for Mt0895 (a recently characterized thioredoxin from *M. thermoautotrophicum*) and *E. coli* thioredoxin. It has been demonstrated that *E. coli* thioredoxin is reduced extremely slowly by NADPH, GSH, and glutathione reductase (*55*). The activity of Mt0807 is however much lower than those observed for T4 glutaredoxin and *E. coli* glutaredoxin. The weak glutaredoxin activity observed for Mt0807 could be due to some hydrophobic binding to glutathione and the high oxidative properties that it exhibits.

DISCUSSION

Sequence and Structure Comparison. Sequence comparison between Mt0807 and "standard" thioredoxins/glutaredoxins (Figure 3) indicate that only a few residues are fully conserved. As a rule, the active site sequence -Trp−Cys−Gly−Pro−Cys- is highly conserved in the thioredoxins where as the glutaredoxins have the conserved -Cys−Pro−Tyr−Cys- sequence in their active site (*20*). On the basis of its sequence alone, Mt0807 would be expected to behave like a glutaredoxin. Furthermore, the structure of Mt0807 clearly shows that it has a glutaredoxin-like fold. Typically, a glutaredoxin fold is similar to a thioredoxin-like fold except that the N-terminal residues (forming a $\beta-\alpha$ secondary structure) are truncated. However, more detailed structural comparisons with other members of the thioredoxin superfamily indicate that the general fold, even though similar to that of glutaredoxin, has several characteristics more common to a thioredoxin. Furthermore, biochemical tests suggest Mt0807 functions much more like a thioredoxin.

Submission of the representative structure to search for structure neighbors in the DALI, CE, SCOP, and PDB databases yielded very useful results. Table 2 lists the summary of the top hits from a SCOP database search. These same hits were also among the top hits in the CE, PDB, and Dali databases. The structures were assessed by their Z scores, alignment length, and RMSD values. Interestingly, the top hits from all these searches were from Archaebacteria with Mt0807's paralogue, Mt0895 topping the list and Mj0307 (its othologue) in second place. These were followed by the glutaredoxins and then bacteriophage T4 glutaredoxin. At the bottom of the list were either the thioredoxins or glutathione transferases. These results indicate that even though Mt0807 is a true thioredoxin, its overall fold is closer to the glutaredoxins than the thioredoxins, suggesting (in addition to other evidence discussed below) that it may be ancestral to the glutaredoxins.

While these fold comparisons are useful for understanding the possible evolution or phylogeny of archaebacterial thioredoxins, it is also important to emphasize that more detailed structural comparisons can help explain Mt0807's observed activity. In particular, the similarities between Mt0807 and other known thioredoxins in terms of the length and orientation of $helix_2$, the loop connecting $helix_2$ and strand β_3, the presence of a glycine residue at the C-terminal end of strand β_4 and the hydrophobic pocket on the surface of the molecule—all of these features are key determinants for thioredoxin reductase binding (*48*), which is observed for Mt0807. Additional structural comparisons between Mt0807 and known glutaredoxins show that Mt0807 lacks the positively charged residues at the opposite sides of its redox-active disulfide bridge which are thought to be essential to glutaredoxin activity.

Thiol Ionization by UV Spectroscopy. The thiol ionization test performed clearly gave results that are consistent with those observed for *E. coli* thioredoxin and with other archaeabacterial thioredoxins. The structure of Mt0807 obtained by NMR shows that the active site cysteines (Cys13 and Cys16) are in a loop between strand-β_1 and α-helix 1 (Figure 2b). Cysteine 13 is exposed, while cysteine 16 is buried. As observed for *E. coli* thioredoxin, the −SH group of Cys13 is expected to be neutralized prior to Cys16 as the pH is increased (*9*). Thus, for *E. coli* thioredoxin, the pK_a's for the exposed and buried cysteines have been reported to be 7.1 and 9.9, respectively (*42*). In glutaredoxins, the pK_a of the exposed cysteine is typically below 5 (those of thioredoxins are above 6.5), while the buried cysteine typically has a pK_a above 9 as in thioredoxins (*58*−*60*). It has also been found that the ionization of the active site thiols is significantly affected by the presence of other charged groups in the molecule. In *E. coli*, these groups are Asp26 and Lys57 and when either one or both residues are mutated in *E. coli*, the two thiols either titrate simultaneously with the same pK_a value (*42*, *61*) or titrate at very close/similar pK_a's (*62*). Aspartic acid 26 is completely buried and in close proximity to the active site (the closest approach being the carboxyl group of Asp26 to the sulfur of Cys35 at 5.9 Å in reduced thioredoxin and 5.6 Å in oxidized thioredoxin (*63*)). The function of Lys57 is not completely clear, but it is thought to be a possible hydrogen bond donor or salt bridge partner for the Asp 26 carboxyl group (*42*). The pK_a of thioredoxins/glutaredoxins is also influenced by the residues between the active site thiols (*19*).

Structural analysis of the Mt0807 protein shows that neither of these groups (Asp or Lys) is proximal to the sulfur of Cys16. Thus, a two-step endpoint with very similar pK_a's or a single pK_a for both thiols would be expected (as was observed). The pK_a value of 6.23 for both thiols is more typical for the exposed cysteine of thioredoxins than for glutaredoxins (*64*, *65*). Our thiol titration result is in close agreement with the published value of an orthologous protein (Mj0307) from *Methanococcus jannaschii* (pK_a 6.27) with which Mt0807 has 51% sequence identity (*19*). Our results also agree closely with the value (6.7) obtained for its paralogue, Mt0895. The low pK_a value is also consistent with

the strong oxidative properties shown by Mt0807 in the thioredoxin activity test (*8*, *19*).

Thioredoxin Activity. The thioredoxin activity test used here allows the two steps involved in the reaction to be monitored separately. Thus, one may ascertain which step is taking place and which is not. The first part of the reaction involves the binding and interaction with thioredoxin reductase, and our results clearly indicate that this step is taking place for all the four proteins used in the experiment. This observation confirms the thioredoxin-like nature of Mt0807 and the extent of the oxidation seen here (which is quite high) is in close agreement with what would be expected on the basis of results recently published by Mossner et al. (*8*). These workers demonstrated that when the dipeptide sequence between the active site cysteines in a thioredoxin is mutated from the wild type (-Cys−Gly−Pro−Cys-) to those of a glutaredoxin (-Cys−Pro−Tyr−Cys-), a protein disulfide isomerase (-Cys−Gly−His−Cys-), or a DsbA (-Cys−Pro−His−Cys-), all the variants proved to be stronger oxidants than the wild type (*8*). The order of oxidizing strength was reported to be glutaredoxin-type > DsbA-type > PDI-type > wild-type with the most oxidizing mutant having the lowest pK_a value for the exposed active site cysteine (pK_a of 5.9). A similar result (*73*) was obtained when the Pro in the dipeptide sequence between the active site cysteines in *E. coli* was mutated to His to mimic that of PDI (protein disulfide isomerase). The mutagenized thioredoxin had an increased redox potential resulting in significant increase in ability to serve as a substrate for thioredoxin reductase and a decrease in its ability to reduce protein disulfides (*73*). The active site sequence of Mt0807 is the same as that of a glutaredoxin (-Cys−Pro−Tyr−Cys-), so it is not surprising that Mt0807 exhibits strong oxidizing activity. The second step in the reaction, a reduction step, is almost nonexistent for Mt0807 as compared to the control proteins. This is expected for a molecule which is such a strong oxidant. This result may also explain why Mt0807 from *M. thermoautrophicum* (Strain Marburg) was originally reported as not being a substrate for thioredoxin reductase (*10*). In all the thioredoxin/thioredoxin reductase assays used by McFarlan and co-workers (*10*), it was the reduction step, not the binding step, which was measured.

Glutaredoxin Activity. To more fully understand the apparent glutaredoxin activity in Mt0807, it is perhaps worthwhile reviewing what is known about a much better characterized glutaredoxin − *E. coli* glutaredoxin. *E. coli* glutaredoxin activity is attributed to residues 12−13 in the active site (Pro−Tyr), 59−60 (Val−Pro), and 69−71 (Gly−Gly−Tyr), which form a hydrophobic surface on one side of the redox-active site. This hydrophobic surface has been suggested to be the binding site for glutathione and other proteins for the redox reaction (*47*). It is also postulated that Arg8, Lys18, and Asp19 in *E. coli* glutaredoxin, which are located at the opposite sides of the redox active disulfide bridge, may be involved in the actual redox process. An Asp residue located at the N-terminus of the third helix in *E. coli* glutaredoxin is also found in most glutaredoxins (*20*). These charged residues, which are all near the active site, have been implicated in the specific participation of ionic interactions with glutathione (*66*, *67*). The structure of Mt0807 shows similar positions of equivalent residues which may form the same hydrophobic binding surface (residues 15−16 of the active site (Pro−Tyr), 56−57 (Val−Pro), 67−69 (Phe−Val−Gly)). However, Mt0807 lacks the positively charged residues at the opposite sides of the redox-active disulfide bridge which are thought to be essential in the actual redox process. In our assays, Mt0807 exhibited some oxidation of glutathione; however, this was small compared to that of *E. coli* glutaredoxin and T4 glutaredoxin. The low level of glutathione oxidation which was observed could be attributed to nonspecific binding of glutathione and the intrinsic oxidative ability of Mt0807. Glutathione is essential for glutaredoxin function and a literature search revealed that most archaeabacteria, including *M. thermoautotrophicum* do not contain glutathione or a glutathione-like cystolic thiols (*10, 19, 20*). Since glutathione has not been isolated in this organism, it seems reasonable to suggest that the activity obtained was perhaps more an artifact of its structural or sequential similarity to glutaredoxin than its evolved function. However, it could also be argued that this activity is an early precursor toward glutaredoxin activity.

Functional Relationship between Mt0807 and Mt0895. An important question that may be asked is why does a simple archaeon like *M. thermoautotrophicum* have two thioredoxins? It is important to note that most eubacteria and all eukaryotes have both a thioredoxin and a glutaredoxin encoded in their genomes. This redundancy in redox function for these organisms may have arisen because the activities sustained by glutaredoxin and thioredoxin (DNA synthesis, transcriptional control, and protein function regulation) are so vital to an organism's viability (*74*). The same may be true for *M. thermoautotrophicum* and other archeons, too.

Structural characterization and biochemical assay comparisons between Mt0807 and Mt0895 indicate that both proteins have similar structures, and both use the same reducing system (the thioredoxin system). Mt0807 is, however, more oxidative and seem to have very little reductive ability as compared to Mt0895. Evidence suggests that Mt0807 is the much more abundant protein in *M. thermoautotrophicum*, especially when grown under native-like anaerobic conditions (*10*). The strong reducing environment in which this organism thrives (*19*) suggests the need for a strongly oxidizing form of thioredoxin to provide the reducing equivalents to ribonucleotide reductase for DNA synthesis. It appears that Mt0807 fits the bill. In contrast, Mt0895 which is the less abundant protein may be a "back-up" to Mt0807 or it may be involved in other, less important disulfide redox activities within the cytoplasm. Alternately, Mt0895 may be the thioredoxin produced when *M. thermoautotrophicum* is exposed to more aerobic conditions.

While both Mt0895 and Mt0807 are true thioredoxins, in some respects, Mt0807 seems to play the role of a glutaredoxin (with its strong oxidizing potential and other physical features), while Mt0895 seems to play the role of a thioredoxin. Given the "archaic" nature of Archea and their hypothesized role in eubacterial and eukaryotic evolution, we would suggest that Mt0807 and Mt0895 may be molecular "fossils" representing an early branch point in the evolution of glutaredoxins and thioredoxins. One could speculate that Mt0807 (or a related ancient variant) maintained its size, shape, and active site residues but changed certain adjacent charged residues to become a glutaredoxin, while Mt0895 (or a related ancient variant) lengthened and slightly changed its active site to become a more effective

thioredoxin. The dual characteristics (thioredoxin-like and glutaredoxin-like) shown by Mt0807, such as the sequence and active site similarities to glutaredoxins (*10*), overall structure similarity to glutaredoxins, but with structural details and enzymology more akin to thioredoxins, are all factors that would seem to support this assertion. Glutathione (GSH) is known to be absent in *M. thermoautotrophicum* (*10*, *19*, *20*); however, it is widely distributed in high concentrations (0.1−10 mM) in animal tissues, plants, and microorganisms (*75*, *76*). It might be that when glutathione became more abundant 1−2 billion years ago, Mt0807-like proteins may have evolved toward a glutaredoxin-like function, using GSH to provide the reducing equivalents for ribonucleotide reductase for DNA synthesis. The relatively small number of residue changes (i.e., two positively charged residues around the active site) that may be needed to convert Mt0807 to a fully functional glutaredoxin (*10*) suggests that the evolutionary process may have been relatively quick and facile.

CONCLUSION

This project was undertaken to clarify/identify the possible redox role of Mt0807. Earlier workers had found conflicting evidence about the possible functions for this protein and had suggested that Mt0807 may be part of a distinct ribonucleotide-reducing system involving ferredoxins and ferredoxin-thioredoxin reductases (*10*). This suggestion arose because of the apparent inactivity between Mt0807 and thioredoxin reductase. Using an improved, two-part thioredoxin reductase assay, we have shown that Mt0807 does indeed interact with thioredoxin reductase. In addition, functional and structural comparisons of Mt0807 to an orthologous (51% identity) thioredoxin from *M. jannaschi* as well as detailed analysis of its own surface topology indicate that Mt0807 is indeed a true thioredoxin and that it belongs to the thioredoxin-thioredoxin reductase system of redox proteins. To further confirm this assessment, we have conducted sequence searches against the *M. thermoautotrophicum* genome to attempt to identify possible ferredoxin-thioredoxin homologues and have found no significant ($E < 0.0\ 1$) hits. This evidence strongly indicates that Mt0807 is not part of a distinct ribonucleotide-reducing system as had been postulated earlier. However, the unusual activity, sequence, and structure of Mt0807 (and its paralogue Mt0895) have led us to speculate that these two molecules may represent a group of ancient proteins that were ancestral to both thioredoxins and glutaredoxins.

ACKNOWLEDGMENT

We wish to thank Cheryl Arrowsmith and Adelinda Lee of the OCI for providing the Mt0807 gene. Thanks also to Trent C. Bjorndahl and Haiyan Zhang for their advice and assistance in the initial NMR analysis. We also wish to thank the International Council for Canadian Studies (ICCS) for providing financial support for one of the authors (G.Y.A.) and also the Protein Engineering Network of Centres of Excellence (PENCE) for providing funding for the project.

SUPPORTING INFORMATION AVAILABLE

PDB coordinates for 1NHO. This material is available free of charge via the Internet at http://pubs.acs.org.

REFERENCES

1. Dalton, T. P., Shertzer, H. G., and Puga, A. (1999) *Annu. Rev. Pharmacol. Toxicol. 39*, 67−101.
2. Holmgren, A. (1989) *J. Biol. Chem. 264*, 13963−13966
3. Jordan, A., and Richard, P. (1998) *Annu. Rev. Biochem. 67*, 71−98.
4. Arner, E. S. J., and Holmgren, A. (2000) *Eur. J. Biochem. 267*, 6102−6109.
5. Jordan, A., Pontis E., Aslund, F., Hellman, U., Gigert, I., and Reichard, P. (1996) *J. Biol. Chem. 271*(15), 8779−8785.
6. Martin, J. L. (1995) *Structure 3*, 245−250.
7. Holmgrem, A. (1995) *Structure 3*, 239−243.
8. Mossner, E., Huber-Wunderlich, M., and Glockshuber, R. (1998) *Protein Sci. 7*(5), 1233−1244.
9. Kallis, G. B., and Holmgren, A. (1980) *J. Biol. Chem. 255*, 10261−10265.
10. McFarlan, S. C., Terrell, C. A., and Hogenkamp, P. C. (1992) *J. Biol. Chem. 267*, 10561−10569.
11. Smith, D. R., Doucette-Stamm, L. A., Deloughery, C., Lee, H., Dubois, J., Aldredge, T., Bashirzadeh, R., Blakely, D., Cook, R., Gilbert, K., Harrison, D., Hoang, L., Keagle, P., Lumm, W., Pothier, B., Qiu, D., Spadafora, R. Vicaire, R., Wang, Y., Wierzbowski, J., Gibson, R., Jiwani, N., Caruso, A., Bush, D., and Reeve, J. N. (1997) *J. Bacteriol. 179*, 7135−7155.
12. Kawarabayasi, Y., Sawada, M., Horikawa, H., Haikawa, Y., Hino, Y., Yamamoto, S., Sekine, M., Ogura, K., Otsuka, R., Nakazawa, H., Takamiya, M., Ohfuku, Y., Funahashi, T., Tanaka, T., Kudoh, Y., Yamazaki, J., Kushida, N., Oguchi, A., Aoki, K., and Kikuchi, H. (1998) *DNA Res. 5*, 147−177.
13. Klenk, H. P., Clayton, R. A., Tomb, J. F., White, O., Nelson, K. E., Ketchum, K. A., Dodson, R. J., Gwinn, M., Hickey, E. K., Peterson, J. D., Richardson, D. L., Kerlavage, A. R., Graham, D. E., Kyrpides, N. C., Fleischmann, R. D., Quack-enbush, J., Lee, N. H., Sutton, G. G., Gill, S., Kirkness, E. F., Dougherty, B. A., Mckenny, K., Adams, M. D., Loftus, B., and Venter, J. C. (1997) *Nature 392*, 353−358.
14. Kawarabayasi, Y., Hino, Y., Horikawa, H., Yamazaki, S., Haikawa, Y., Jin-no, K., Taakahashi, M., Sekine, M., Baba, S., Ankai, A., Kosugi, H., Hosoyama, A., Fukui, S., Nagai, Y., Nishijima, K., Nakazawa, H., Takamiya, M., Masuda, S., Funahashi, T., Tanaka, T., Kudoh, Y., Yamazaki, J., Kushida, N., Oguchi, A., and Kikuchi, H. (1999) *DNA Res. 6*, 83−101.
15. Deckert, G., Warren, P. V., Gaasterland, T., Young, W. G., Lenox, A. L., Graham, D. E., Overbeek, R., Snead, M. A., Keller, M., Aujay, M., Huber, R., Feldman, R. A., Short, J. M., Olsen, G. J., and Swanson, R. V. (1998) *Nature 392*, 353−358.
16. Nelson, K. E., Clayton, R. A., Gill, S. R., Gwinn, M. L., Dodson, R. J., Haft, D. H., Hickey, E. K., Peterson, J. D., Nelson, W. C., Ketchum, K. A., McDonald, L., Utterback, T. R., Malek, J. A., Linher, K. D., Garrett, M. M., Stewart, A. M., Cotton, M. D., Pratt, M. S., Phillips, C. A., Richardson, D., Heilderberg, J., Sutton, G. G., Fleischmann, R. D., Eisen, J. A., and Fraser, C. M. (1999) *Nature 399*, 323−329.
17. Bult, C. J., White, O., Olsen, G. J., Zhou, L., Fleischmann, R. D., Sutton, G. G., Blake, J. A., Fitzgerald, L. M., Clayton, R. A., Gocayne, J. D., Kerlavage, A. R., Doughgherty, B. A., Tomb, J. F., Adams, M. D., Reich, C. I., Overbeek, R., Kirkness, E. F., Weinstock, K. G., Merrick, J. M., Glodek, A., Scott, J. L, Geoghagen, N. S. M., and Venter, J. C. (1996) *Science 273*, 1058−1073.
18. Jordan, A., Aslund, F., Pontis, E., Reichard, P., and Holmgren, A. (1997) *J. Biol. Chem. 272*(29), 18044−18050.
19. Lee, D. Y., Ahn, B.-Y., and Kim, K.-S. (2000) *Biochemistry 39*, 6652−6659.
20. Bhattacharyya, S., Habibi-Nazhad, B., Amegbey, G., Slupsky, C. M., Yee, A., Arrowsmith, C., and Wishart D. S. (2002) *Biochemistry 41*, 4760−4770.
21. Stehr, M., Schneider, G., Aslund, F., Holmgren, A., and Lindquist, Y. (2001) *J. Biol. Chem. 276*(38) 35836−35841.
22. *The QIAexpressionist, A Handbook for High-Level Expression and Purification of 6x His-Tagged Proteins*, 5th ed., March 2001, pp 63−73, QIAGEN.
23. Jeener, J., Meier, B. H., Bachmann, P., and Ernst, R. R. (1979) *J. Chem. Phys. 71*, 4546−4553.
24. Kay, L. E., Keifer, P., and Saarinen, T. (1992) *J. Am. Chem. Soc. 114*, 10663−10665.
25. Zhang, O., Kay, L. E., Olivier, J. P., and Forman-Kay, J. D. (1994) *J. Biomol.* NMR *4*, 845−858.

26. Kuboniwa, H., Grzesiek, S., Delagio, F., and Bax, A. (1994) *J. Biomol. NMR 4*, 871−878.
27. Kay, L. E., Xu, G. Y., and Yamazaki, T. (1994) *J. Magn. Reson. Ser. A 109*, 129−133.
28. Wishart, D. S., and Case, D. A., (2001) *Methods Enzymol. 338*, 3−34.
29. Wishart, D. S., and Sykes, B. D. (1994) *Methods Enzymol. 239*, 363−392.
30. Brunger, A. T. (1993) *X-PLOR Manual, Version 3.851*, Yale University, New Haven, CT.
31. Nilges, M., Gronenborn, A. M., Brunger, A. T., and Clore, G. M. (1988) *Protein Eng. 2*, 27−38.
32. Nigles, M., Clore, G. M., and Gronenborn, A. M. (1988) *FEBS Lett. 229*, 317−324.
33. Wuthrich, K. (1986) *NMR of Proteins and Nucleic Acids*, John Wiley and Sons Inc., New York.
34. Nilges, M., Kuszewski, J., and Brunger, A. T. (1991) In *Computational Aspects of the Study of Biological Macromolecules by NMR* (Hoch, J. C., Ed.) New York, Plenum Press.
35. Kuszewski, J., Nilges, M., and Brunger, A. T. (1992) *J. Biomol. NMR 2*, 33−56.
36. Garrett, Kuszewski, J., Hancock, Lodi, Vuister, Gronenborn, A. M., and Clore, G. M. (1994) *J. Magn. Reson. Ser. B 104*, 99−103.
37. Kuszewski, J., Qin, Gronenborn, A. M., and Clore, G. M. (1995) *J. Magn. Reson. Ser. B 106*, 92−106.
38. Kuszewski, J., Gronenborn, A. M., and Clore, G. M. (1995) *J. Magn. Reson. Ser.* B *107*, 293−297.
39. Laskowski, R. A., Rullmann, J. A. C., MacArthur, M. W., Kaptein, R., and Thornton, J. (1996) *J. Biomol. NMR 8*, 477−486.
40. Wishart, D. S., Willard, L., and Sykes, B. D. (1995) University of Alberta, (http://redpoll.pharmacy.ualberta.ca).
41. Koradi, R., Billeter, M., and Wuthrich, K. (1996) *J. Mol. Graphics 14*, 51−55.
42. Dyson, J. H., Jeng, M.-F, Tennant, I. S., Lindell, M., Cui, D.-S., Kuprin, S., and Holmgren, A. (1997) *Biochemistry 30*, 2622−2636.
43. Holmgren, A. (1979) *J. Biol. Chem. 254*, 3664−3671.
44. Wang, Y. Ph.D. Thesis (1999) University of Alberta, Edmonton, Alberta.
45. Cave, W. J., Cho, S. H., Batchelder, M. A., Yokota, H., Kim, R., and Wemmer, E. D. (2001) *Protein Sci. 10*, 384−396.
46. Lennon, B. W., Williams, C. H., Jr., and Ludwig, M. L. (2000) *Science 289*, 1190−1194.
47. Eklund, H., Cambillau, C., Sjoberg, B. M., Holmgren, A., Jornvall, H., Hoog, J. O., and Branden, C. I. (1984) *EMBO J. 3*, 143−1449.
48. Holmgren, A., Kallis, G. B., and Nordstrom, B. (1981) *J. Biol. Chem. 256*, 3118−3124.
49. Russel, M., and Model, P. (1986) *J. Biol. Chem. 261*, 14997−15005.
50. Polgar, L. (1974) *FEBS Lett. 38*, 189−190.
51. Nelson, J. W., and Creighton, T. E. (1994) *Biochemistry 33*, 5974−5983.
52. Benesch, R. E., and Benesch, R. (1995) *J. Am. Chem. Soc. 77*, 5877−5881.
53. Holmgren, A., and Bjornstedt, M. (1995) *Methods Enzymol. 252*, 1999−208.
54. Waksman, G., Krishna, T. S. R., Williams, C. H., and Kuriyan, J. (1994) *J. Mol. Biol. 236*, 800.
55. Holmgren, A. (1978) *J. Biol. Chem. 253*, 7424−7430.
56. Szajewski, R. P., and Whitesides, G. M. (1980) *J. Am. Chem. Soc. 102*, 2011−2026.
57. Holmgren, A. (1979) *J. Biol. Chem. 254*, 3672−3678.
58. Takahashi, N., and Creighton, T. E. (1996) *Biochemistry 35*, 8342−8353.
59. Gan, Z. R., Polokoff, M. A., Jacobs, J. W., and Sardana, M. K. (1990) *Biochem. Biophys. Res. Commun. 168*, 944−951.
60. Mieyal, J. J., Starke, D. W., Gravina, S. A., and Hocevar, B. A. (1991) *Biochemistry 30*, 8883−8891.
61. Vohnik, S., Hanson, C., Tuma, R., Fuchs, J. A., Woodward, C., and Thomas, G. J., Jr. (1998) *Protein Sci. 7*, 193−200.
62. Wilson, N. A., Barbar, E., Fuchs, J. A., and Woodward, C. (1995) *Biochemistry 34*, 8931−8939.
63. Jeng, M. F., Holmgren, A., and Dyson, H. J. (1995) *Biochemistry 34*, 10101−10105.
64. Gan, Z. R., and Wells, W. W. (1987) *J. Biol. Chem. 262*, 6704−6707.
65. Sun, C. H., Berardi, M. J., and Bushweller, J. H. (1998) *J. Mol. Biol. 280*, 687−701.
66. Nordstrand, K., Aslund, F., Holmgren, A., Otting, G., and Berndt, K. D. (1999) *J. Mol. Biol. 286*, 541−552.
67. Berardi, J. M., and Bushweller, J. H. (1999) *J. Mol. Biol. 292*, 151−161.
68. Holm, L., and Sander, C. (1993) *J. Mol. Biol. 233*, 123−138.
69. Holm, L., and Sander, C. (1996) *Science 273*, 595−602.
70. Murzin, A. G., Brenner, S. E., Hubbard, T., and Chothia, C. (1995) *J. Mol. Biol. 247*, 536−540.
71. Shindyalov, I. N., and Bourne, P. E. (1998) *Protein Eng. 11*, 739−747.
72. Altschul, S. F., Madden, T. L., Schaffer, A. A., Zhang, J., Zhang, Z., Miller, W., and Lipman, D. J. (1997) *Nucleic Acid Res. 25*, 3389−3402.
73. Krause, G., Lundstrum, J., Barea, J. L., Pueyo de la Cuesta, C., and Holmgren, A. (1991) *J. Biol. Chem. 266*, 9494−9500.
74. Holmgren, A. (1985) *Annu. Rev. Biochem. 54*, 237−271.
75. Meister, A. (1988) *J. Biol. Chem. 263*, 17205−17208.
76. Fuchs, J. A. (1989) In *Glutathione: Chemical, Biochemical, and Medical Aspects* (Dolphin, D., Poulsen, R., and Avramovic, O., Eds.) Part B, pp 551−570, John Wiley and Sons, New York.
77. Christendat, D., Yee, A., Dharamsi, A., Kluger, Y., Savchenko, A., Cort, J. R., Booth, V., Mackereth, C. D., Saridakis, V., Ekiel, I., Kozlov, G., Maxwell, K. L., Wu. N., McIntosh, P., Gehring, K., Kennedy, M. A., Davidson, A. R., Pai, F. E., Gerstein, M., Edwards, A. M., and Arrowsmith, C. H. (2000) *Nat. Struct. Biol. 7*, 903−909.
78. Yee, A., Chang, X., Pineda-Lucena, A., Wu, B., Semesi, A., Le, B., Ramelot, T., Lee, G. M., Bhattacharyya, S., Gutierrez, P., Denisov, A., Lee, C.-H., Cort, J. R., Kozlov, G., Liao, J., Finak, G., Chen, L., Wishart, D., Lee, W., McIntosh, L. P., Gehring, K., Kennedy, M. A., Edwards, A. M. and Arrowsmith, C. H. (2002) *Proc. Nat. Acad. Sci. U.S.A. 99*, 1825−1830.

BI030021G